ORIGINAL PAPER

Differentiation-specific association of HP1α and HP1β with chromocentres is correlated with clustering of TIF1β at these sites

Eva Bártová · Jiří Pacherník · Alois Kozubík · Stanislav Kozubek

Abstract Mammalian heterochromatin protein 1 (HP1α, HP1β, HP1γ subtypes) and transcriptional intermediary factor TIF1β play an important role in the regulation of chromatin structure and function. Here, we investigated the nuclear arrangement of these proteins during differentiation of embryonal carcinoma P19 cells into primitive endoderm and into the neural pathway. Additionally, the differentiation potential of trichostatin A (TSA) and 5-deoxyazacytidine (5-dAzaC) was studied. In 70% of the cells from the neural pathway and in 20% of TSA-stimulated cells, HP1α and HP1β co-localized and associated with chromocentres (clusters of centromeres), which correlated with clustering of TIF1β at these heterochromatic regions. The cell types that we studied were also characterized by a pronounced focal distribution of HP1γ. The above-mentioned nuclear patterns of HP1 and TIF1β proteins were completely different from the nuclear patterns observed in the remaining cell types investigated, in which HP1α was associated with chromocentres while HP1β and HP1γ were largely localized in distinct nuclear regions. Moreover, a dispersed nuclear distribution of TIF1β was observed. Our findings showed that the nuclear arrangement of HP1 subtypes and TIF1β is differentiation specific, and seems to be more important than changes in the levels of these proteins, which were relatively stable during all the induced differentiation processes.

Keywords HP1 proteins · TIF1β · Chromocentres · Differentiation · Embryonal carcinoma cells

Introduction

Mammalian heterochromatin protein 1 (HP1) (Eissenberg and Elgin 2000) belongs to the class of non-histone proteins that are involved in regulation of chromatin remodelling and transcription. In mammalian cells, three HP1 subtypes (HP1α, HP1β, HP1γ) are characterized by distinct nuclear distributions: HP1α mainly associates with the centromeres of interphase nuclei; HP1β is associated with centromeres to a lesser extent; and HP1γ is often concentrated in euchromatic loci or in both euchromatin and heterochromatin compartments (Horsley et al. 1996; Minc et al. 1999; Nielsen et al. 2001; Li et al. 2002). HP1 proteins also bind to the centromeric regions of metaphase chromosomes (Minc et al. 1999, 2001; Yamada et al. 1999); however, the consistent localisation of HP1 proteins at metaphase centromeres has not been observed, as this appears to depend on the cell types and antibodies used (Wreggett et al. 1994; Minc et al. 1999, 2000, 2001; Saffery et al. 1999). More precise analyses revealed that specific molecular domains of HP1α and HP1β are responsible for their association with metaphase and interphase centromeres. Moreover, in some cell lines, it was found that all three HP1 subtypes could be localised to both clusters of centromeres (described by

E. Bártová (✉) · A. Kozubík · S. Kozubek
Institute of Biophysics,
Academy of Sciences of the Czech Republic,
Královopolská 135, 612 65 Brno, Czech Republic
e-mail: bartova@ibp.cz

J. Pacherník · A. Kozubík · S. Kozubek
Department of Animal Physiology and Immunology,
Institute of Experimental Biology, Faculty of Science,
Masaryk University in Brno, Kotlářská 2, 611 37 Brno,
Czech Republic

Alcobia et al. 2000 as chromocentres) and promyelocytic leukaemia (PML) nuclear bodies, but with different preferences (Everett et al. 1999; Hayakawa et al. 2003).

HP1 proteins are also thought to be important structural elements associated with heterochromatin-mediated gene silencing (Ekwall et al. 1995; Kellum and Alberts 1995; Yamaguchi et al. 1998). Several transcriptional regulators have the ability to bind HP1 proteins and thereby silence genes (Nielsen et al. 1999, 2001; Ryan et al. 1999; Lechner et al. 2000). An example is the mammalian transcriptional intermediary factor TIF1β. Co-immunoprecipitation experiments revealed that TIF1β interacts with all HP1 subtypes, which was documented in undifferentiated embryonal carcinoma P19 cells (Nielsen et al. 1999). Co-localisation of both TIF1β and HP1α proteins with centromeres was found to be required for the induction of the parietal and visceral endoderm differentiation pathways (Cammas et al. 2002, 2004). This interaction was probably involved in heterochromatin-mediated gene silencing (Cammas et al. 2004), as observed for the sequence-specific transcription factor *Ikaros*, which also associates with centromeres during lymphoid differentiation (Brown et al. 1997, 1999). This well-known epigenetic silencing mechanism, known as position effect variegation (PEV) in *Drosophila*, has been reviewed by Eissenberg et al. (1990), and is responsible for the silencing of euchromatic loci close to heterochromatic domains (Wakimoto 1998).

It is well known that all HP1 subtypes consist of a chromodomain (CD) and a chromoshadow domain (CSD) that are separated by hinge regions (Aasland and Stewart 1995; Bannister et al. 2001; Cowell et al. 2002; Jacobs and Khorasanizadeh 2002; Li et al. 2002; Muchardt et al. 2002). The chromodomain of HP1s is highly selective for histone H3 methylated at lysine 9 (K9) (summarised by Rice and Allis 2001; Cowell et al. 2002). Therefore, the association of HP1 subtypes with chromocentres corresponds to the fact that pericentromeric regions are enriched with trimethylated H3(K9) (summarised by Rice and Allis 2001; Lachner et al. 2003). These observations imply that HP1 proteins, H3(K9) methylated regions and chromocentres contribute to functionally and structurally important nuclear compartments that, in addition, can influence the transcriptional activity of euchromatic loci (summarised by Lachner et al. 2003).

To understand the differentiation-specific relationships between HP1-TIF1β interphase patterns, and the affinity of these proteins for chromocentres, we have studied several differentiation pathways of embryonal carcinoma P19 cells. These cells are a pluripotent murine embryonal carcinoma cell line that has been widely used as a model system for studying the early events of embryonic differentiation. Embryonal carcinoma P19 cells resemble the inner cell mass of the early embryo and can differentiate into various cell types according to the culture conditions in vitro. This cell population can also form chimeras after injection into mouse blastocysts (McBurney 1993; Andrews 2002). Treatment of these cells with retinoic acid (RA; 0.1–1 μM) in the presence of serum leads to highly homogeneous differentiation into primitive endoderm; however, neuroectoderm/neural cells are clearly visible when the serum is absent (Jones-Villeneuve et al. 1982; Pacherník et al. 2005). Recently, these cells were used as a convenient model for studies of HP1-mediated heterochromatinisation and HP1 interaction with nucleosomal core histones (Nielsen et al. 2001).

Despite the fact that all variants of HP1 proteins are structurally conserved from yeast to humans (Eissenberg and Elgin 2000), the interphase patterns seem to be cell-type specific (Minc et al. 1999; Taddei et al. 2001; Bártová et al. 2005 and data shown here). In our experiments, we observed the co-localisation of HP1α and HP1β and more condensed foci of HP1γ in the cells from the neural pathway and in approximately 20% of TSA-stimulated embryonal carcinoma P19 cells. Undifferentiated cells, 80% of TSA-treated cells, 5-dAzaC-treated cells and the cells of primitive endoderm were characterised by distinct nuclear positioning of HP1α and HP1β and by a more dispersed distribution of HP1γ and TIF1β. In cells from the neural pathway, co-localisation of HP1α and HP1β corresponded well with the focal distribution of TIF1β close to the chromocentres; however, these structural modifications were not accompanied by pronounced changes in the protein levels. Enhanced accumulation of TIF1β near chromocentres of neural cells could be explained by the ability of TIF1β to bind to both HP1α and HP1β proteins (Nielsen et al. 1999), which co-localised in this cell type. Our data further imply that the nuclear patterns of HP1 proteins, TIF1β and chromocentres are differentiation-specific, and appear to be functionally more important than the protein levels, which remain constant during the induction of differentiation.

Materials and methods

Cell culture and treatments

Mouse embryonal carcinoma P19 cells were purchased from the European Collection of Cell Cultures, Wiltshire, UK. These cells were cultured in tissue culture dishes pre-treated for 10 min with a 0.1% aqueous

solution of gelatine. Dulbecco's modified Eagle's medium (D-MEM) containing 10% fetal calf serum, 0.05 μM β-mercaptoethanol, 100 i.u./ml penicillin, and 0.1 mg/ml streptomycin was used. Under serum-free conditions, the cells were cultured in D-MEM/F12 (1:1) medium supplemented with the ITS supplement and antibiotics as described above (all from GIBCO BRL, Chemos CZ, Prague, Czech Republic). To initiate differentiation, the embryonal carcinoma P19 cells (5×10^3/cm²) were seeded onto the gelatinised tissue culture dishes in complete D-MEM medium, 24 h before the application of experimental conditions.

To induce primitive endoderm differentiation, the cells were cultivated in a fresh original medium containing 10% serum and 0.2 μM all-trans retinoic acid (RA; Sigma, Prague, Czech Republic) (S-R). To induce neural differentiation, the original medium was replaced by serum-free media with 0.2 μM RA (SF-R). In both cases, the RA treatment was applied for the first 2 days, and then the RA-containing media were replaced with appropriate media without RA. After two additional days (total of 4 days), the cells turned into primitive endoderm (S-R) and neural (SF-R) cell populations (Pacherník et al. 2005). Embryonal carcinoma P19 cells were also treated with TSA (100 nM) or with 20 μM of 5-dAzaC in complete D-MEM medium for 24 and 48 h, respectively. Control and treated cells were cultivated in standard conditions at 37°C in a humidified atmosphere containing 5% CO_2.

Immunostaining of the interphase nuclei

The cells were fixed on microscope slides with 4% formaldehyde for 10 min at room temperature (RT), permeabilised with both 0.1% Triton X-100 for 8 min and 0.1% saponin for 12 min (Sigma, Germany), and washed twice in PBS for 15 min. We then incubated the preparation in 1% BSA (dissolved in PBS) for 1 h at RT. The slides were washed for 15 min in PBS, and incubated with anti-HP1α (clone 15.19s, #05–689, Upstate, USA), anti-HP1β (#07–333, Upstate, USA), anti-HP1γ (clone 42s2, #05–690, Upstate, USA) and anti-C-terminus of TIF1β (#sc-19168, Santa Cruz, CA). Each antibody was diluted 1:200 (1:100 for TIF1β) in 1% BSA dissolved in PBS, and then incubated overnight at 4°C. The cells were washed twice in PBS for 5 min, and incubated for 1 h with the appropriate secondary antibody. We used anti-rabbit IgG-FITC (#F0511, Sigma, Germany), donkey anti-goat IgG-FITC (#sc-2024, Santa Cruz, CA) and goat anti-mouse IgG₃-Alexa Fluor 594 (Molecular Probes, USA). Secondary antibodies were diluted 1:200 in 1% BSA dissolved in PBS. Immunostained cells were washed three times in PBS for 5 min, and counterstained with DAPI (4′,6-diamidino-2-phenylindole, 0.2 μg/ml) or TO-PRO-3 (0.04 μg/ml) (Molecular Probes, USA). Interphase nuclei were analysed using Nipkow disk confocal microscopy, and 100 nuclei were acquired in three independent experiments.

Image acquisition

The images of immunostained cell nuclei were acquired by a Nipkow disk confocal system consisting of an argon/krypton laser (Innova 70, Coherent) with an acousto-optical tuneable filter (AOTF, Brimrose) for wavelength selection, and a confocal head (QLC 100; VisiTech International) connected to a Leica DMRXA epi-fluorescence microscope (LEICA) with a Piezo-controlled z-movement (Physic Instrumente). The scanning system was driven by FISH 2.0 software (Kozubek et al. 1999) running on a personal computer. The images were captured with a fully programmable digital CoolSnap CCD camera (Photometrix, Tucson, AZ). The magnification of the objective lens was 100× (NA = 1.3). For embryonal carcinoma P19 adherent cells, 70 optical sections, with axial steps of 0.1 μm, were scanned. Three-dimensional projections were done using Andor iQ software (ANDOR Technology, version 1.0.1). The average distances of chromocentres (the weight centre of each chromocentre was calculated) from the nuclear weight centre, normalised to the local nuclear radius, were calculated using FISH 2.0 software according to Bártová et al. (2005). The data from the FISH 2.0 analysis were exported to Sigma Plot 8.0 software (Jandel Scientific, California) to perform the final mathematical evaluation. Statistical analysis was performed using the bio-statistical software Statistica (StatSoft, Czech Republic) and tested for conformity to a normal distribution. As our results were pronouncedly asymmetric and did not correspond to normal distributions, the Mann–Whitney U test was applied to all data. Asterisks (shown in Fig. 6f) indicate statistically significant differences from the control value at the level $P \geq 0.05$.

Western blotting

Cells were washed with PBS and lysed in sodium dodecyl sulphate (SDS)-lysis buffer (50 mM Tris–HCl, pH 7.5; 1% SDS; 10% glycerol). The protein concentrations were determined using the DC Protein assay kit (Bio-Rad, Bio-Consult, Czech Republic). Lysates were supplemented with bromophenol blue (0.01%) and β-mercaptoethanol (1%), and equal amounts of total proteins (10 μg) were subjected to SDS-PAGE. After being elec-

trotransferred onto a polyvinylidene difluoride membrane (Immobilon-P, Sigma, Czech Republic), proteins were immuno-detected using appropriate primary and secondary antibodies and visualised by ECL + Plus reagent (Amersham Pharmacia Biotech, Czech Republic) according to the manufacturer's instructions. The following primary antibodies were employed: anti-HP1α (clone 15.19s2, #05–689, Upstate, USA), anti-HP1β (#07–333, Upstate, USA), anti-HP1γ (clone 42s2, #05–690, Upstate, USA), rabbit polyclonal antibody against total histone H3 (#06–755, Upstate, USA), anti-acetyl-H3(K9) (#06–942, Upstate, USA) and anti-C-terminus of TIF1β (#sc-19168, Santa Cruz, CA). The level of lamin B was studied using an appropriate goat polyclonal antibody (#sc-6217, Santa Cruz, CA). The levels of differentiation markers such as Oct-4, Endo-A and IIIβ-tubulin were determined using the following antibodies: mouse monoclonal antibody against Oct-3/4 (C10) (#sc-5279, Santa Cruz, CA), rat monoclonal antibody against mouse endoderm-specific cytokeratin Endo-A (TROMA-I, Developmental Studies Hybridoma Bank, University of Iowa) and mouse monoclonal antibody against human neuron-specific class IIIβ-tubulin isotype, which cross reacts with the mouse homologue (TU-20, provided by Pavel Dráber, Institute of Molecular Genetics, Prague, Czech Republic). After immuno-detection, each membrane was stained with amidoblack to confirm equal protein loading.

Agarose gel electrophoresis

Genomic DNA was isolated from control and 5-dAzaC-treated cells using the Blood & Cell Culture DNA Mini kit (#13323, Qiagen, Bio-Consult, Czech Republic), and 1 μg DNA was digested with 375 units of methylation-sensitive *Hpa*II restriction enzyme. Incubation was for 16 h at 37°C. The reaction was stopped by heat inactivation for 20 min at 65°C. The DNA fragments were separated by electrophoresis on 0.9% NuSieve agarose gel (Cambrex, USA) and stained with ethidium bromide (1 μg/ml).

Transfection of cells with an expression vector encoding GFP-HP1

Individual plasmids encoding GFP-HP1α, GFP-HP1β and GFP-H1γ (a generous gift from the Laboratory of Receptor Biology and Gene Expression, the National Institutes of Health, Bethesda, USA) were inserted into *Escherichia coli* DH5α for amplification. Plasmid DNA was isolated by Qiagen Large-Construct kit (#12462, Qiagen, Bio-Consult, Czech Republic) and this purified DNA was used for electroporation of embryonal

carcinoma P19 cells as described by Pacherník et al. (2005). These experiments were performed to compare nuclear patterns of exogenously expressed GFP-HP1 proteins with patterns of endogenous HP1s.

Results

Characteristics of differentiation pathways of mouse embryonal carcinoma P19 cells

The morphology of embryonal carcinoma P19 cells was studied in progenitor cell population (Fig. 1a), after TSA and 5-dAzaC treatments (Fig. 1b, c) and during selected differentiation pathways (SR in panel d and SF-R in panel e). As can be seen in Fig. 1a, undifferentiated embryonal carcinoma P19 cells grew in compact colonies, clearly visible under the light microscope. In comparison with these control cells, TSA induced a fibroblast-like cell shape (Fig. 1b), while 5-dAzaC-treated cells adopted a more flattened shape (Fig. 1c). In the next experiments, the well-defined protocols for differentiation of embryonal carcinoma P19 cells (Pacherník et al. 2005) were used. After RA treatment in the presence of serum (S-R) (Fig. 1d), the cell population became more flattened and the cells were dispersed on the surface of the culture dishes, while RA alone in the absence of serum induced the neural morphology (SF-R) (Fig. 1e). Cell differentiation into primitive endoderm (S-R in Fig. 1d) was additionally verified by the detection of primitive endoderm-specific markers such as cytokeratin Endo-A (Fig. 1f), and a high level of neuron-specific IIIβ-tubulin was observed in neural cells (Fig. 1g). The analysis of differentiation markers by Western blotting (Fig. 1h) revealed high levels of Oct-4 protein (used as a marker of pluripotency) in undifferentiated embryonal carcinoma P19 cells, while both S-R and SF-R differentiation pathways were characterised by a lack of Oct-4. Testing the level of Oct-4 in the cells treated with TSA and 5-dAzaC, we observed a remarkable decrease in Oct-4 with TSA treatment and a slight reduction after 5-dAzaC treatment. These findings indicate that TSA, and to some extent 5-dAzaC, may have some differentiation potential; however, loss or decrease in Oct-4 (see Fig. 1h) does not necessarily imply that TSA and 5-dAzaC have differentiation activity.

Histone hyperacetylation and DNA hypomethylation induced in embryonal carcinoma P19 cells

The effect of TSA, as an inhibitor of histone deacetylases (HDACi), on the histone acetylation state was
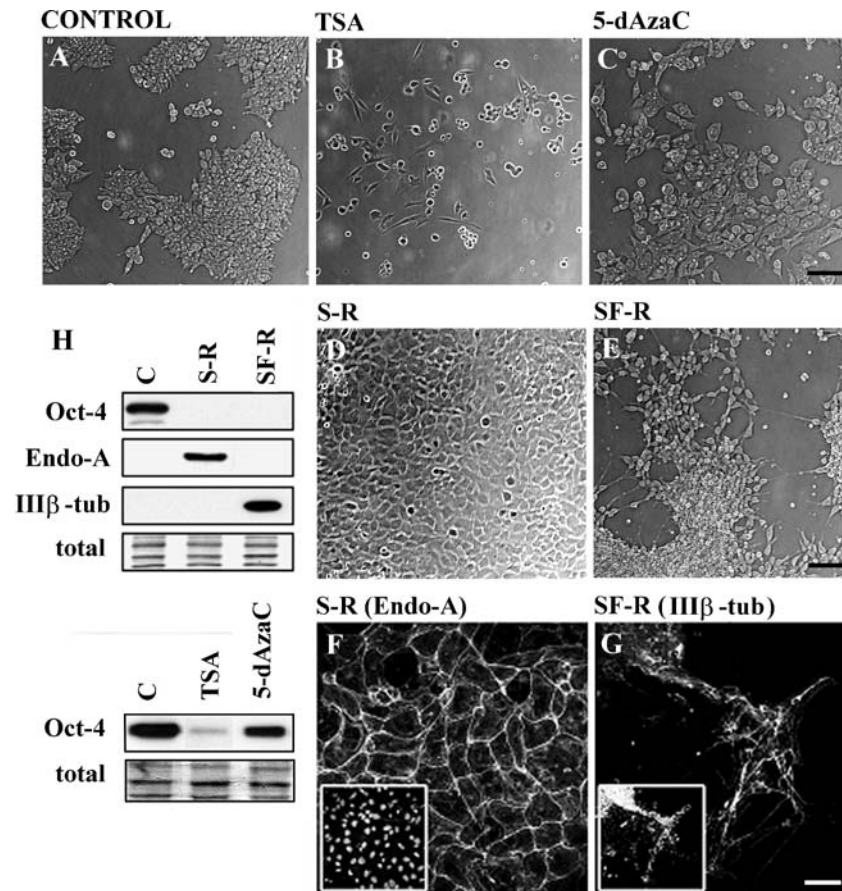
Fig. 1 Morphology of embryonal carcinoma P19 cells studied during histone hyperacetylation, DNA hypomethylation and during endoderm and neural differentiation pathways. **a** Control mouse embryonal carcinoma P19 cells growing in clusters. **b** Embryonal carcinoma P19 cells treated with the HDAC inhibitor TSA were characterised by fibroblast-like morphology. **c** DNA hypomethylation by 5-dAzaC induced a flattened morphology. **d** Four days of cell cultivation with retinoic acid, dissolved in medium with serum (*S-R*), induced an endodermal phenotype. **e** Retinoic acid in medium without serum (*SF-R*) induced a neural population. **f** To verify the specific differentiation pathway, cytokeratin Endo A (*Endo-A*), a specific primitive endoderm factor, was labelled in S-R cells. Staining of cell nuclei with DAPI is shown in the insert. **g** IIIβ-tubulin is a characteristic marker of neural populations. The presence of IIIβ-tubulin was verified using immunocytochemistry. Staining of cell nuclei by DAPI is shown in the insert. **h** Differentiation markers such as Oct-4, Endo-A and IIIβ-tubulin were analysed by Western blotting, and the levels of all proteins were normalised to the total protein levels

verified by Western blotting. In comparison with the control, an extensive TSA-dependent increase in H3(K9) acetylation was observed, accompanied by a slight decrease in the level of histone H3 (Fig. 2a).

DNA demethylating effects of 5-dAzaC were demonstrated by enhanced cleavage of total genomic DNA with *Hpa*II restriction enzyme. *Hpa*II is sensitive to cytosine methylation at CCGG recognition sites. In the absence of *Hpa*II we observed intact, high molecular weight DNA on agarose gels (Fig. 2b). After *Hpa*II restriction, a pronounced low-molecular-weight DNA fraction became visible in the samples from 5-dAzaC-treated embryonal carcinoma P19 cells (Fig. 2b).

Additionally, we tested the level of acetylated H3(K9) and the total level of H3 in 5-dAzaC-treated cells, and in endoderm and neural populations. No changes in the levels of acetylated H3(K9) and histone H3 were found in the S-R and SF-R differentiation pathways (Fig. 2a). However, after 5-dAzaC treatment, we observed a decreased level of acetylated H3(K9), probably as a consequence of the reduced level of total histone H3 (Fig. 2a).

Distribution of HP1 proteins in nuclei of undifferentiated embryonal carcinoma P19 cells

A number of cell types similar to embryonal carcinoma P19 cells are characterised by co-localisation of HP1α with chromocentres (Everett et al. 1999; Hayakawa et al. 2003). Formation of chromocentres was also

Fig. 2 Histone and DNA methylation analyses. **a** Changes in global histone H3(K9) acetylation and levels of total histone H3 after TSA and 5-dAzaC treatments, and during S-R and SF-R differentiation of embryonal carcinoma P19 cells. Data from Western blotting were normalised to the total nuclear protein levels. Triplicate experiments using Western blotting were performed and the representative results are shown in panel **a**. **b** Agarose gel analysis of non-restricted (−) and *Hpa*II-restricted (+) genomic DNA isolated from the control and from 5-dAzaC-treated embryonal carcinoma P19 cells. Hypomethylated DNA is shown after 5-dAzaC treatments as a low-molecular weight smear
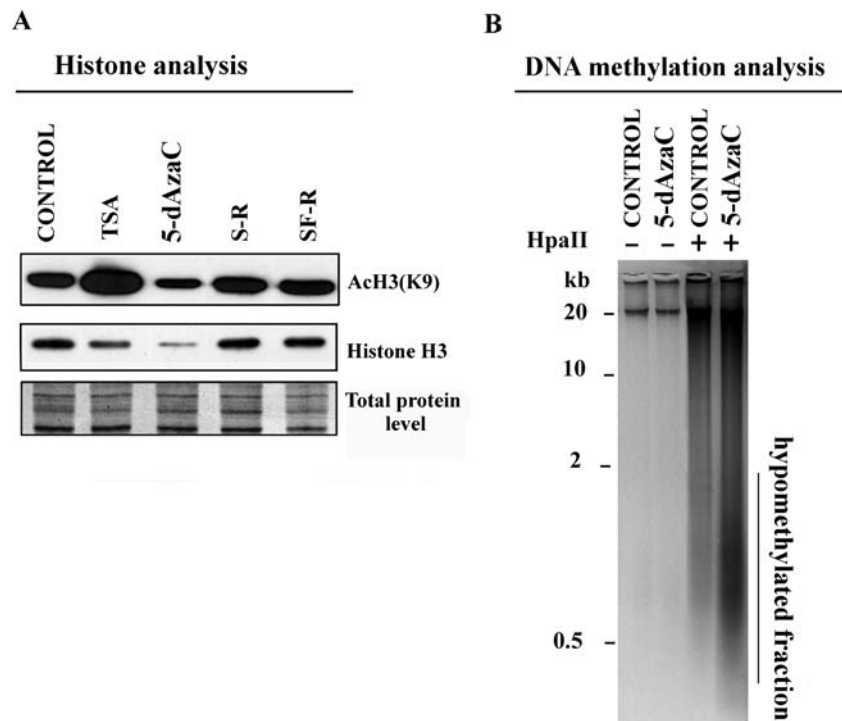
observed in embryonal carcinoma P19 cells after DAPI counterstaining (Fig. 3a, e, i). Densely stained chromocentres were associated with 100% of HP1α foci, as shown in Fig. 3a and b (merged in Fig. 3c, see insert). Focal distribution of HP1α was also observed in cells transiently expressing GFP-HP1α, but to a lesser extent (Fig. 3d).
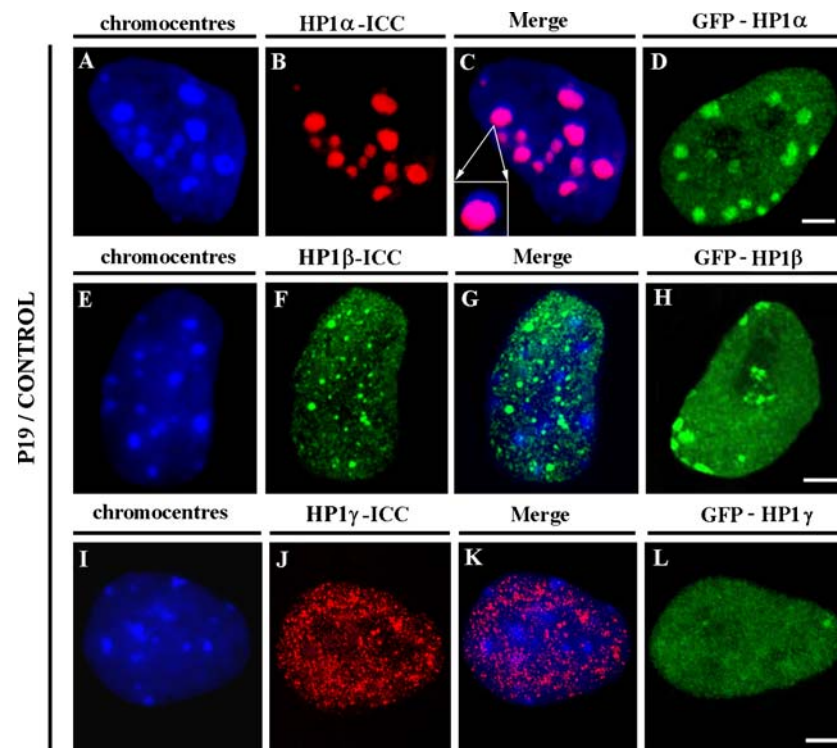
Immunocytochemical analyses of undifferentiated embryonal carcinoma P19 cells revealed relatively fine foci of endogenous HP1β (Fig. 3f, g), which did not strictly co-localise with chromocentres (Fig. 3g). In these cells, fine foci were also found for the third HP1 subtype, HP1γ (Fig. 3j, k), that preferentially localised outside chromocentres, probably in euchromatic regions (Fig. 3k). Comparing nuclear patterns of endogenous HP1β and HP1γ proteins with patterns of the same but exogenously expressed nuclear components, we observed certain differences. Contrary to the results from immunocytochemistry, we found a high level of GFP fluorescence, not appearing as fine foci (Fig. 3h, l). Significant differences were also revealed between large foci of exogenously expressed GFP-HP1α and both exogenously expressed GFP-HP1β and GFP-HP1γ (compare Fig. 3d with Fig. 3h and l).

HP1α and HP1β co-localised during neural differentiation

Dual immunocytochemistry was performed to study the interrelationship between nuclear localisation of HP1α and HP1β. In undifferentiated embryonal carcinoma P19 cells, in the majority of cells treated with TSA or 5-dAzaC, and in the S-R-stimulated population, HP1α and HP1β did not co-localise; this was also clearly visible in 3D-lateral projections (Fig. 4a). Pronounced co-localisation of HP1α and HP1β was observed in approximately 95% of HP1 foci in embryonal carcinoma P19 cells induced to neural differentiation (Fig. 4a, P19/SF-R panel). This is documented by 3D projections of the cell from the neural pathway (P19/SF-R) and by separated images of HP1α and HP1β in the same cell (red foci of HP1α are shown in the upper P19/SF-R panel and green foci of HP1β are shown in the lower P19/SF-R panel). The co-localisation of HP1α and HP1β was observed in approximately 70% of SF-R and in 20% of TSA-treated embryonal carcinoma P19 cells (Fig. 4e). Therefore, the relationship between HP1α and HP1β proteins with chromocentres was more precisely analysed only in SF-R-stimulated cell populations (Fig. 4b). Both HP1α and HP1β subtypes associated with chromocentres; however, an exact co-localisation of HP1 proteins with chromocentres was not observed (see magnifications in Fig. 4b, inserts).

HP1γ nuclear localisation was studied in control, TSA- and 5-dAzaC-treated embryonal carcinoma P19 cells, and during the S-R and SF-R differentiation pathways (Fig. 4c). The interphase profile of HP1γ was conserved after the majority of treatments, but not after SF-R cell stimulation, where a pronounced

Fig. 3 Immunocytochemical analyses of HP1α, HP1β and HP1γ proteins in undifferentiated embryonal carcinoma P19 cells. **a** DAPI staining was used to show chromocentres. **b** HP1α formed distinct foci in embryonal carcinoma P19 cells. **c** HP1α (*red*) associated with chromocentres; see also higher magnification (see *insert*). **d** Embryonal carcinoma P19 cell, transiently expressing GFP-HP1α. **e** Chromocentres in a embryonal carcinoma P19 cell stained with DAPI. **f** HP1β was organised into fine foci, shown by immunocytochemistry. **g** Overlay image of chromocentres (*blue* foci) and HP1β (*green*). **h** Embryonal carcinoma P19 cell transiently expressing GFP-HP1β. **i** Chromocentres in a control embryonal carcinoma P19 cell stained with DAPI. **j** Nuclear pattern of HP1γ visualised by immunocytochemistry and confocal microscopy. **k** Overlay of chromocentres (*blue* foci) and HP1γ (*red*). **l** Embryonal carcinoma P19 cell transiently expressing GFP-HP1γ. *Scale bar* indicates 0.5 μm

focal arrangement of HP1γ was found (Fig. 4c, SF-R). In these cells, the association of HP1γ with chromocentres was revealed in approximately 35% of HP1γ foci (see example in Fig. 4b, red arrows and frame with red arrow), while the rest of this protein was apparently positioned in euchromatic regions of neural cells (Fig. 4b, white arrows and magnification in HP1γ panel of Fig. 4b). After TSA treatment, approximately 20% of cells were characterised by the presence of several larger foci of HP1γ (Fig. 4c, white arrow); however, these regions were not so distinct when compared with the neural pattern (Fig. 4c, compare TSA with SF-R). Our data imply that unlike the neural pathway, TSA has an ability to induce a heterogeneously differentiated population of embryonal carcinoma P19 cells.

Analysing the levels of all three HP1 subtypes by Western blotting, we have observed highly stable protein levels during all treatments tested (Fig. 4d). A slightly reduced level of HP1γ was only found after TSA cell stimulation (Fig. 4d).

Changes of HP1α pattern in the 'cell-anchorage region' after TSA and 5-dAzaC treatments

A part of the cell nucleus, in close association with the cell attachment to the culture dish ('cell anchorage region'), was densely occupied by HP1α (Fig. 4a). It was observed especially in control embryonal carcinoma P19 cells. TSA and 5-dAzaC caused relocation of HP1α foci from this nuclear region (Fig. 4a, TSA and 5-dAzaC, lateral projections). In primitive endoderm cells as well as in SF-R-treated cells, we did not observe this effect (Fig. 4a, SR and SF-R). Except in control cells, we found that apoptosis was occurring, as shown by cleavage of lamin B (65 kDa) to 45 kDa fragments (Fig. 4d). In TSA- and 5-dAzaC-treated populations, detachment of cells from culture dishes was more frequently observed than in S-R and SF-R differentiated cells (light microscope observation). On the other hand, lamin B cleavage was less intense in the adherent population of TSA- and 5-dAzaC-treated cells than after S-R and SF-R treatments (documented in
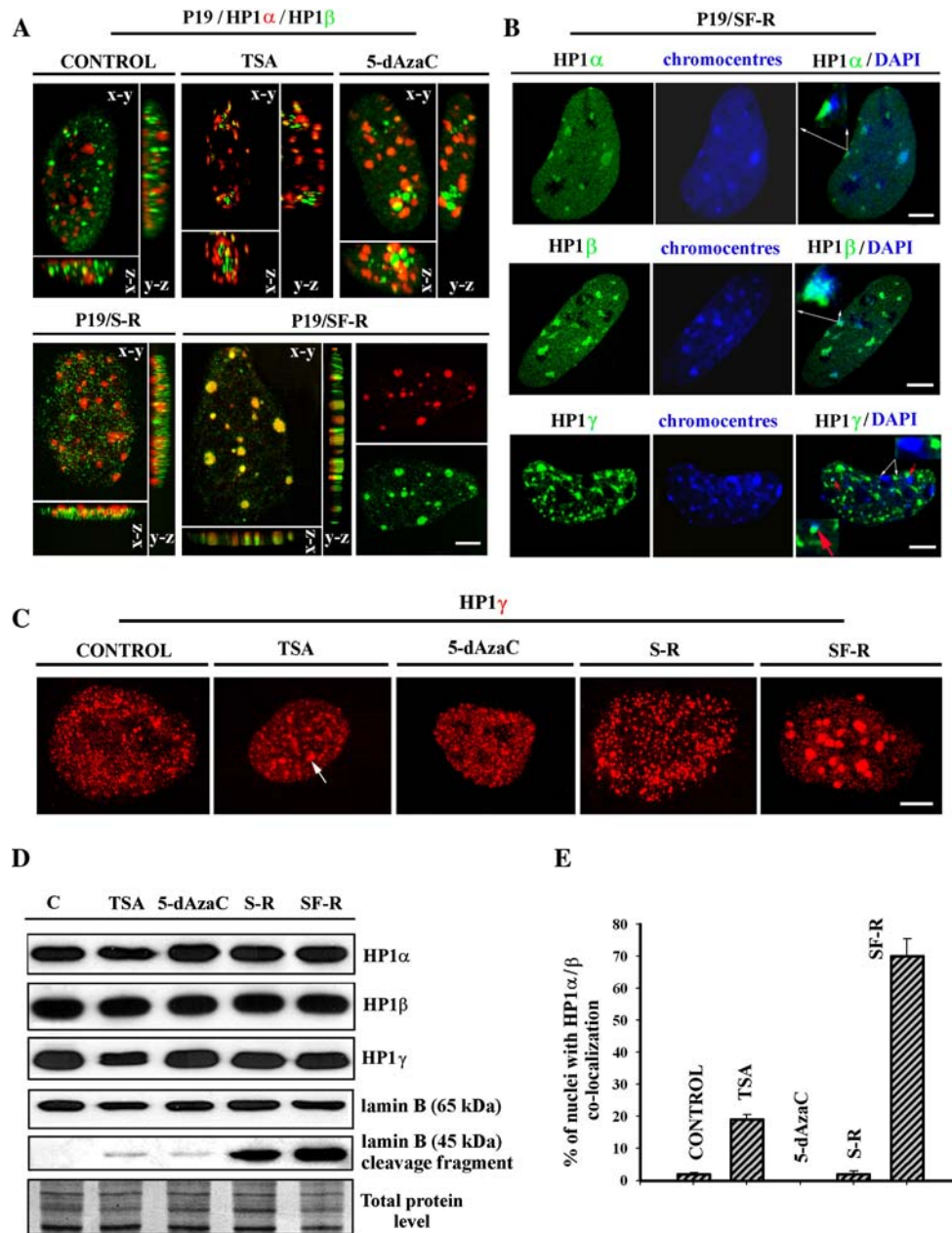
Fig. 4 **a** Detection of HP1α and HP1β using dual immunostaining in undifferentiated, TSA-treated and 5-dAzaC-treated cells, and in embryonal carcinoma P19 cells induced to endoderm (S-R) and to the neural pathway (SF-R). Maximum images (*x-y*) are shown for each treatment and lateral projections (*x-z*, *y-z*) are included with each panel. Structural changes were observed after TSA and 5-dAzaC treatments at the regions of cell adherence to culture surfaces. Cells induced to neural differentiation, and 20% of TSA-stimulated cells, (panel **e**) were characterised by co-localisation of HP1α and HP1β, unlike control and 5-dAzaC-treated cells and cells stimulated to form endoderm. **b** Analyses of HP1 protein co-localisation with chromocentres were performed in embryonal carcinoma P19 cells differentiated into the neural lineage: HP1α and HP1β were chromocentres associated with in approximately 95% of foci (see higher magnification, *insert*). In the neural population, HP1γ was located in both euchromatic and heterochromatic compartments; HP1γ was associated with chromocentres in approximately 35% of foci (*red arrows* and *insert* with *red arrow*). *White arrows* show separate positioning of one chromocentre (*blue*) and one HP1γ region (*green*). *Scale bars* indicate 1 μm. **c** Nuclear pattern of HP1γ in embryonal carcinoma P19 cells treated with TSA or 5-dAzaC, or stimulated to endoderm and neural cell differentiation. *Scale bar* indicates 1 μm. **d** Levels of HP1α, HP1β and HP1γ proteins and lamin B (65 kDa) cleavage into 45 kDa fragments (longer exposure than for 65 kDa lamin B fragment has been used) were detected in embryonal carcinoma P19 cells stimulated with TSA or 5-dAzaC, or induced to endoderm and neural cell maturation. Results in the undifferentiated (control) cell population are labelled as '*C*'. **e** This panel represents the percentage of nuclei with HP1α/HP1β co-localisation, which was evaluated after all the different treatments of embryonal carcinoma P19 cells (approximately 100 nuclei for each treatment were analysed)

Fig. 5 Immunocytochemical analyses of transcriptional intermediary factor TIF1β. **a** Nuclear pattern of TIF1β in undifferentiated, TSA-treated and 5-dAzaC-treated embryonal carcinoma P19 cells, and in endoderm and neural cell populations. *Scale bar* indicates 1.5 μm. **b** Analysis of the TIF1β protein level in all cell types studied was performed using Western blotting. TIF1β protein levels were normalised to the total protein levels. **c** Percentage of nuclei with focal TIF1β arrangement in progenitor, TSA-treated and 5-dAzaC-stimulated embryonal carcinoma P19 cells, and in the same cells induced to endoderm (S-R) and neural (SF-R) differentiation pathways
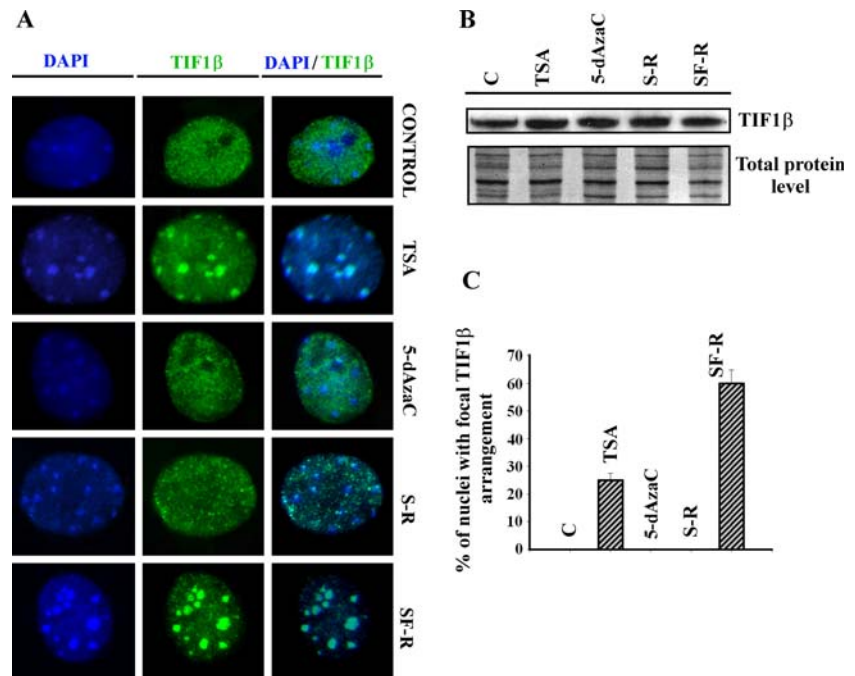

Fig. 4d). The occurrence of apoptosis during all the differentiation pathways tested excluded an influence of this process on repositioning of HP1α from the nuclear compartment in close proximity to 'cell anchorage regions'. Therefore, relocation of HP1α to the nuclear interior seems to be an effect of hyperacetylation or DNA hypomethylation induced by the inhibitors tested.

## Nuclear distribution and levels of TIF1β transcriptional intermediary factor

It is well known that HP1-TIF1β interaction is essential for the induction of specific differentiation pathways of mouse embryonal carcinoma cells (Cammas et al. 2002, 2004). To contribute to the knowledge of the role of TIF1β in differentiation processes, we also studied the nuclear pattern of TIF1β in embryonal carcinoma P19 cells treated with TSA or 5-dAzaC, or induced into the primitive endoderm and neural differentiation pathways (Fig. 5a). Using confocal immunofluorescence microscopy, we observed that TIF1β is diffusely distributed throughout the nucleoplasm of undifferentiated and 5-dAzaC-treated cells (Fig. 5a). However, approximately 25% of TSA-stimulated cells were characterised by a focal arrangement of TIF1β in close association with chromocentres (Fig. 5a, TSA and 5c). In cells induced into primitive endoderm, we did not observe a focal arrangement of TIF1β (Fig. 5a). However, a pronounced focal distribution of TIF1β, associated with the chromocentres, was observed in

approximately 60% of the cells induced into the neural pathway (SF-R in Fig. 5a, c). Levels of TIF1β were shown to be stable by Western blotting in all cases tested (Fig. 5b).

A reduced number of chromocentres was observed during induction of differentiation pathways

In parallel with changes in focal localisation of HP1 proteins, a reduced number of chromocentres was observed in all cell types studied (Fig. 6a–e). These experiments were performed to investigate chromocentre rearrangement during induced differentiation, which also in some cases strongly reflects HP1α nuclear reorganisation in particular. In control cells, approximately 20 centromeric clusters per cell were found (Fig. 6a), whereas cells treated with TSA displayed an average of only nine chromocentres per cell (Fig. 6b). Interestingly, in approximately 15% of TSA-treated cells, no visible chromocentres were detected (Fig. 6b zero bar, and DAPI staining in TSA panel of Fig. 6f). In 5-dAzaC-treated cells, we found 16.5 ± 0.4 chromocentres (Fig. 6c), and a similar average number of chromocentres per cell was found for both S-R and SF-R differentiated cells (Fig. 6d, e). The average distances of chromocentres from the nuclear weight centre, normalised to the local nuclear radius, were additionally calculated for all cell types tested (see values in abbreviations in Fig. 6f showing average chromocentre location as a percentage of the nuclear radius ± standard errors). Using quantitative
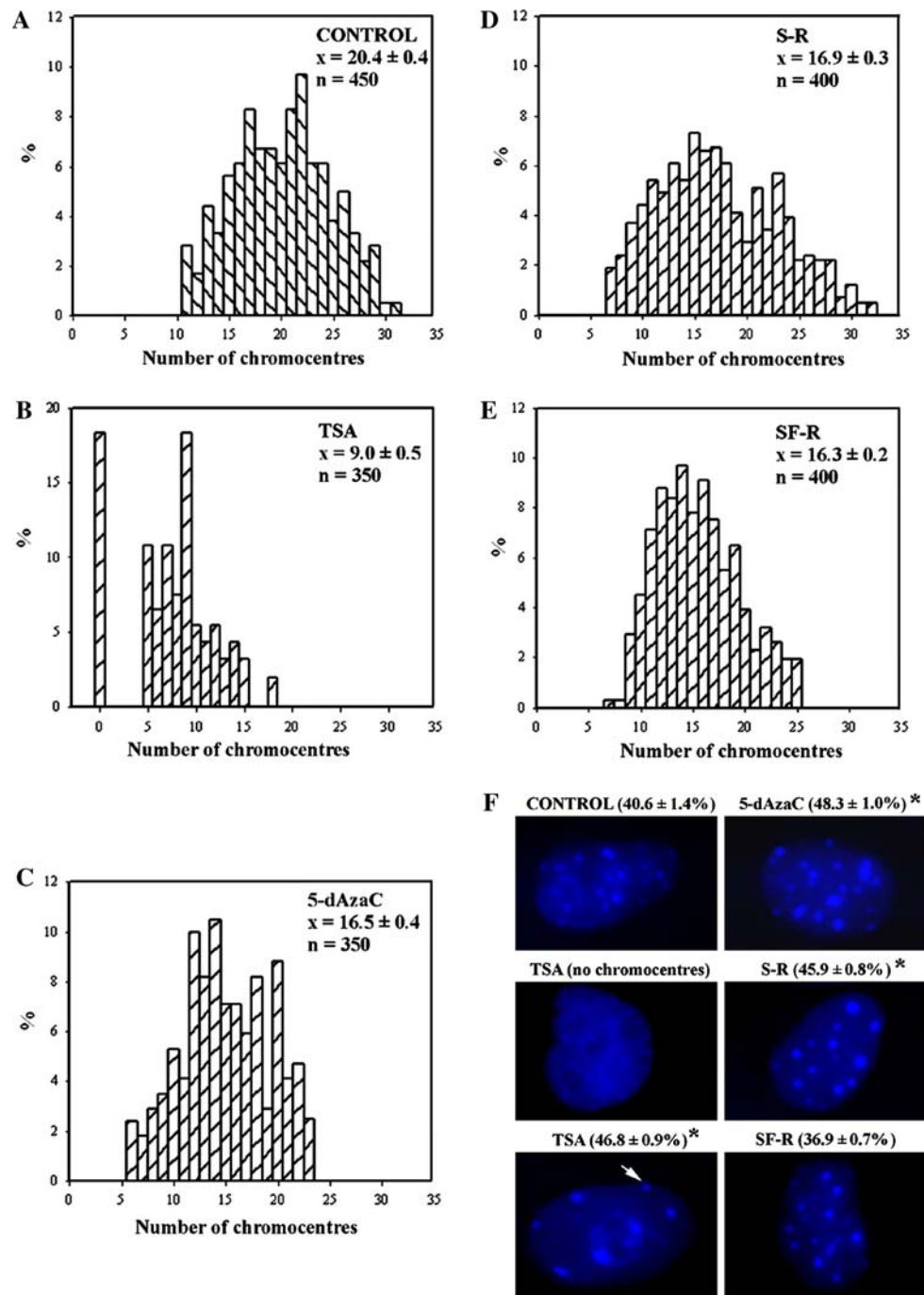
Fig. 6 Nuclear arrangement of chromocentres in embryonal carcinoma P19 cells. The number of chromocentres was evaluated in approximately 350–400 nuclei each of undifferentiated (**a**), TSA-treated (**b**) and 5-dAzaC-treated (**c**) cells, and in embryonal carcinoma P19 cells induced to endoderm (S-R) (**d**) and neural (SF-R) (**e**) differentiation. No visible chromocentres were found in 15% of TSA-treated cells, as determined by DAPI staining (**f**). In undifferentiated cells, approximately 20 chromocentres were observed, while 5-dAzaC, S-R and SF-R treatments reduced the number of chromocentres to approximately 16. The cells treated with TSA displayed an average of only nine chromocentres per cell. The nuclear arrangement of chromocentres after DAPI staining, and the average distances of chromocentres from the nuclear weight centre (normalised to the local nuclear radius), are shown in panel **f**. The Mann–Whitney *U*-test was applied to all data, and *asterisks* indicate results that are statistically significant, different from the control value at the level $P \geq 0.05$

image analysis, we observed the relocation of chromocentres closer to the nuclear membrane in TSA- and 5-dAzaC-treated cells, and in the S-R-stimulated cell population. However, no statistically significant repositioning of chromocentres was observed for the neural cell types (Fig. 6f).

Discussion

Present studies on the understanding of the structural and functional properties of chromatin are often based on analyses of heterochromatin/euchromatin formation and its relationship to the repression or stimulation of fundamental nuclear and cellular processes. In our experiments, we have studied the nuclear arrangement of all the variants of heterochromatin protein 1 (HP1) and of transcriptional intermediary factor TIF1β and the nuclear distribution of chromocentres during cell differentiation and after cell stimulation by inhibitors of HDACs and DNA methyltransferases. We have used mouse embryonal carcinoma P19 cells, which represent a well-established model system for early embryonic development and cellular differentiation (McBurney 1993; Andrews 2002). We used retinoic acid as a powerful differentiation agent that in the presence or absence of serum induced primitive endoderm or neural maturation (Jones-Villeneuve et al. 1982; Pacherník et al. 2005). In our experiments, we also found that both TSA and 5-dAzaC have the ability to stimulate differentiation, deduced from the decreased level of Oct-4 (Fig. 1h), which is considered an important marker of stem cell pluripotency (e.g. Hay et al. 2004; Wiblin et al. 2005).

HP1-TIF1β-chromocentre interaction during mouse embryonal carcinoma cell differentiation

Interaction of TIF1β with all members of the HP1 protein family was first described by Nielsen et al. (1999). In these experiments, all three HP1s were found in the TIF1β immunoprecipitate obtained from undifferentiated embryonal carcinoma P19 cells. Differentiation-specific compartmentalisation of TIF1β at centromeric regions, dependent on a mechanism involving HP1α-TIF1β interaction, was described by Cammas et al. (2002). This interaction was not essential for the differentiation of mouse F9 embryonal carcinoma cells into the primitive endoderm, but was required for induction of subsequent cell maturation in parietal and visceral endoderm (Cammas et al. 2004). In these experiments, the authors tested the nuclear patterns of HP1α-TIF1β, but they did not address the nuclear arrangement of HP1β and HP1γ subtypes. In our experiments, we have observed that a focal arrangement of TIF1β close to chromocentres appears only in cells characterised by a pronounced association of HP1α/HP1β with chromocentres. These observations imply that this nuclear pattern should be important for compartmentalisation of TIF1β at these heterochromatic regions. It could also be explained as a consequence of an increased number of molecules of HP1 proteins at chromocentres, which manifests itself as a focal accumulation of TIF1β that can bind to both HP1α and HP1β proteins (Nielsen et al. 1999). Our data support the conclusion that HP1α and HP1β directly interact and influence each other (Verschure et al. 2005). These interactions probably affect the nuclear arrangement of TIF1β, as shown here.

In our experiments, cells induced to form primitive endoderm were characterised by fine spots of TIF1β, and no co-localisation of HP1α and HP1β was found (Figs. 4a, 5a,). Conversely to Cammas et al. (2002), a focal arrangement of TIF1β was not observed in this type of differentiation. This could be explained by the fact that distinct cell types were induced into similar differentiation pathways, or by the fact that the HP1–TIF1β interaction is not essential for primitive endoderm maturation (Cammas et al. 2004). However, the importance of HP1–TIF1β association was pointed out for parietal and visceral endoderm, and for differentiation into cardiomyocytes and neural cell types (Cammas et al. 2002). It was also shown in our model of neural maturation and, therefore, the results described imply that not only HP1–TIF1β interactions, but also nuclear patterns of the HP1 subtypes and compartmentalisation of TIF1β at chromocentres, play an essential role in the induction of some differentiation processes.

Cell-type specific pattern of HP1 proteins

Here, we observed cell-type specific patterns and nuclear compartmentalisation of HP1 (α, β and γ) proteins (Fig. 4). In comparison with Minc et al. (1999), who reported strict co-localisation of HP1α and HP1β in mouse 3T3 cells but not in HeLa cells, we have found distinct nuclear distributions of HP1α and HP1β in undifferentiated embryonal carcinoma P19 cells, 5-dAzaC-treated cells and in endoderm cells. Co-localisation of these foci was found in a neural cell population (Fig. 4a, P19/SF-R), and in approximately 20% of TSA-stimulated cells. Cell-type specific patterns of HP1 proteins were also documented by Gilbert et al. (2003), who reported high levels of HP1s in embryonic erythrocytes of mouse, while during differentiation of the erythrocytes of chicken, all HP1 subtypes were completely lost. In addition, Lukášová et al. (2005) observed a similar absence of HP1 proteins in human peripheral blood granulocytes.

The differentiation-related changes in the interphase patterns of HP1 and TIF1β proteins also appeared after TSA treatment (Figs. 4, 5). Pronounced focal accumulation of HP1 proteins after TSA treatment is in agreement with the results of Bártová et al. (2005).

However, in the experiments presented here, TSA-stimulated embryonal carcinoma P19 cells formed a more heterogeneous population, which could be explained as a consequence of hyperacetylation and differentiation being induced together. Unlike the TSA-related decrease in the levels of HP1s, reported by Taddei et al. (2001) and Bártová et al. (2005), we have only observed a slightly reduced level of the HP1γ subtype in TSA-stimulated cells (Fig. 4d). This can only be explained by cell-type specific responses. The effects of TSA were studied in detail in the experiments of Taddei et al. (2001). These authors reported complete dissociation of HP1α into fine spots after 5 days of TSA treatment. However, Bártová et al. (2005) showed more distinct foci for all subtypes of HP1 after 2 days of TSA stimulation. In both reports, HP1α dissociated from chromocentres that were repositioned closer to the nuclear envelope, as was also confirmed by our quantitative image analysis shown in Fig. 6f (TSA panel) and by repositioning of HP1α closer to the nuclear weight centre (Fig. 4a). Total dissociation of HP1α from the chromocentres was observed by Taddei et al. (2001), while Bártová et al. (2005) found this phenomenon only for peripherally located centromeres. On the other hand, Gilchrist et al. (2004) reported stable nuclear positioning of centromeres within interphase nuclei a short time after a high-dose exposure to TSA, and therefore Taddei et al. (2005) discussed the effect of TSA from the point of view of dose and exposure and cell-type specificity.

HP1 proteins and the nuclear periphery

In our experiments, we have tried to provide information about changes in the patterns of HP1 proteins and associated structures during cell differentiation and after inhibition of selected epigenetic processes. Pronounced structural modifications were also found for the nuclear region closely associated with the 'cell anchorage region' to culture surfaces (Fig. 4a, HP1α in TSA and 5-dAzaC-treated cells). The observed nuclear rearrangement seems not to be related to the induction of apoptosis. In our experiments, apoptosis was found during all differentiation pathways tested, and therefore repositioning of HP1α to the nuclear interior could be considered as an effect of histone hyperacetylation induced by TSA, and DNA hypomethylation stimulated by 5-dAzaC. More central repositioning of HP1α after TSA treatment is in good agreement with Bártová et al. (2005), and these results imply that the nuclear compartment in close proximity to the 'cell anchorage region' represents a specific part of the nuclear periphery, and therefore it

should be considered separately in higher-order chromatin analyses.

Taken together, we observed differentiation-specific reorganisation of HP1 proteins and TIF1β, which represent highly dynamic components of chromatin (Cheutin et al. 2003) and are required for the stability of heterochromatin domains and for induction of specific maturation pathways (Cammas et al. 2002, 2004). Differentiation-related nuclear reorganisation also involved the clusters of centromeres, called chromocentres, the formation of which was well described by Alcobia et al. (2000, 2003). The repositioning of chromocentres closer to the nuclear periphery (Fig. 6f) seems to be a general feature of many differentiation pathways (summarised by Bártová and Kozubek 2006) or could be related to the hyperacetylation induced by TSA that is characterised by the dissociation of centromeres and HP1α (Taddei et al. 2001 and Bártová et al. 2005). In our experiments, all cell stimulations led to a decrease in the level of Oct-4 protein, which is considered to be a marker of stem cell pluripotency. Therefore, we can summarise that several differentiation pathways were induced in our experiments with mouse embryonal carcinoma P19 cells. Co-localisation of HP1α and HP1β appeared as an important structural feature, probably necessary for compartmentalisation of these HP1 proteins with TIF1β. Changes in the nuclear patterns and interactions of HP1s and TIF1β were functionally more significant than the protein levels studied, which did not change significantly during the induction of differentiation.

References

Aasland R, Stewart AF (1995) The chromo shadow domain, a second chromo domain in heterochromatin-binding protein 1, HP1. Nucleic Acid Res 23:3168–3173

Alcobia I, Dilao R, Parreira L (2000) Spatial associations of centromeres in the nuclei of hematopoietic cells: evidence for cell-type-specific organizational patterns. Blood 95:1608–1615

Alcobia I, Quina AS, Neves H, Clode N, Parreira L (2003) The spatial organization of centromeric heterochromatin during

normal human lymphopoiesis: evidence for ontogenically determined spatial patterns. Exp Cell Res 90:358–369

Andrews PW (2002) From teratocarcinomas to embryonic stem cells. Philos Trans R Soc Lond B Biol Sci 357:405–417

Bannister AJ, Zegerman P, Partridge JF, Miska EA, Thomas JO, Allshire RC, Kouzarides T (2001) Selective recognition of methylated lysine 9 on histone H3 by the HP1 chromo domain. Nature 410:120–124

Bártová E, Kozubek S (2006) Nuclear architecture in the light of gene expression and cell differentiation studies. Biol Cell 98:323–336

Bártová E, Pacherník J, Harničarová A, Kovařík A, Kovaříková M, Hofmanová J, Skalníková M, Kozubek M, Kozubek S (2005) Nuclear levels and patterns of histone H3 modification and HP1 proteins after inhibition of histone deacetylases. J Cell Sci 118:5035–5046

Brown KE, Guest SS, Smale ST, Hahm K, Merkenschlager M, Fisher AG (1997) Association of transcriptionally silent genes with Ikaros complexes at centromeric heterochromatin. Cell 91:845–854

Brown KE, Baxter J, Graf D, Merkenschlager M, Fisher AG (1999) Dynamic repositioning of genes in the nucleus of lymphocytes preparing for cell division. Mol Cell 3:207–217

Cammas F, Oulad-Abdelghani M, Vonesch JL, Huss-Garcia Y, Chambon P, Losson R (2002) Cell differentiation induces TIF1beta association with centromeric heterochromatin via an HP1 interaction. J Cell Sci 115:3439–3448

Cammas F, Herzog M, Lerouge T, Chambon P, Losson R (2004) Association of the transcriptional corepressor TIF1beta with heterochromatin protein 1 (HP1): an essential role for progression through differentiation. Genes Dev 18:2147–2160

Cheutin T, McNairn AJ, Jenuwein T, Gilbert DM, Singh PB, Misteli T (2003) Maintenance of stable heterochromatin domains by dynamic HP1 binding. Science 299:721–725

Cowell IG, Aucott R, Mahadevaiah SK, Burgoyne PS, Huskisson N, Bongiorni S, Prantera G, Fanti L, Pimpinelli S, Wu R, Gilbert DM, Shi W, Fundele R, Morrison H, Jeppesen P, Singh PB (2002) Heterochromatin, HP1 and methylation at lysine 9 of histone H3 in animals. Chromosoma 111:22–36

Eissenberg JC, Elgin SC (2000) The HP1 protein family: getting a grip on chromatin. Curr Opin Genet Dev 10:204–210

Eissenberg JC, James TC, Foster-Hartnett DM, Hartnett T, Ngan V, Elgin SC (1990) Mutation in a heterochromatin-specific chromosomal protein is associated with suppression of position-effect variegation in Drosophila melanogaster. Proc Natl Acad Sci USA 87:9923–9927

Ekwall K, Javerzat JP, Lorentz A, Schmidt H, Cranston G, Allshire R (1995) The chromodomain protein Swi6: a key component at fission yeast centromeres. Science 269:1429–3141

Everett RD, Earnshaw WC, Pluta AF, Sternsdorf T, Ainsztein AM, Carmena M, Ruchaud S, Hsu WL, Orr A (1999) A dynamic connection between centromeres and ND10 proteins. J Cell Sci 112:3443–3454

Gilbert N, Boyle S, Sutherland H, de Las Heras J, Allan J, Jenuwein T, Bickmore WA (2003) Formation of facultative heterochromatin in the absence of HP1. EMBO J 22:5540–5550

Gilchrist S, Gilbert N, Perry P, Bickmore WA (2004) Nuclear organization of centromeric domains is not perturbed by inhibition of histone deacetylases. Chromosome Res 12:505–516

Hay DC, Sutherland L, Clark J, Burdon T (2004) Oct-4 knockdown induces similar patterns of endoderm and trophoblast differentiation markers in human and mouse embryonic stem cells. Stem Cells 22:225–235

Hayakawa T, Haraguchi T, Masumoto H, Hiraoka Y (2003) Cell cycle behavior of human HP1 subtypes: distinct molecular

domains of HP1 are required for their centromeric localization during interphase and metaphase. J Cell Sci 116:3327–3338

Horsley D, Hutchings A, Butcher GW, Singh PB (1996) M32, a murine homologue of Drosophila heterochromatin protein 1 (HP1), localises to euchromatin within interphase nuclei and is largely excluded from constitutive heterochromatin. Cytogenet Cell Genet 73:308–311

Jacobs SA, Khorasanizadeh S (2002) Structure of HP1 chromodomain bound to a lysine 9-methylated histone H3 tail. Science 295:2080–2083

Jones-Villeneuve EM, McBurney MW, Rogers KA, Kalnins VI (1982) Retinoic acid induces embryonal carcinoma cells to differentiate into neurons and glial cells. J Cell Biol 94:253–262

Kellum R, Alberts BM (1995) Heterochromatin protein 1 is required for correct chromosome segregation in Drosophila embryos. J Cell Sci 108:1419–1431

Kozubek M, Kozubek S, Lukášová E, Marečková A, Bártová E, Skalníková M, Jergová A (1999) High-resolution cytometry of FISH dots in interphase cell nuclei. Cytometry 36:279–293

Lachner M, O'Sullivan RJ, Jenuwein T (2003) An epigenetic road map for histone lysine methylation. J Cell Sci 116:2117–2124

Lechner MS, Begg GE, Speicher DW, Rauscher FJ III (2000) Molecular determinants for targeting heterochromatin protein 1-mediated gene silencing: direct chromoshadow domain-KAP-1 corepressor interaction is essential. Mol Cell Biol 20:6449–6465

Li Y, Kirschmann DA, Wallrath LL (2002) Does heterochromatin protein 1 always follow code? Proc Natl Acad Sci USA 99:16462–16469

Lukášová E, Kořístek Z, Falk M, Kozubek S, Grigoryev S, Kozubek M, Ondřej V, Kroupová I (2005) Methylation of histones in myeloid leukemias as a potential marker of granulocyte abnormalities. J Leukoc Biol 77:100–111

McBurney MW (1993) P19 embryonal carcinoma cells. Int J Dev Biol 37:135–140

Minc E, Allory Y, Worman HJ, Courvalin JC, Buendia B (1999) Localization and phosphorylation of HP1 proteins during the cell cycle in mammalian cells. Chromosoma 108:220–234

Minc E, Courvalin JC, Buendia B (2000) HP1gamma associates with euchromatin and heterochromatin in mammalian nuclei and chromosomes. Cytogenet Cell Genet 90:279–284

Minc E, Allory Y, Courvalin JC, Buendia B (2001) Immunolocalization of HP1 proteins in metaphasic mammalian chromosomes. Methods Cell Sci 23:171–174

Muchardt C, Guilleme M, Seeler JS, Trouche D, Dejean A, Yaniv M (2002) Coordinated methyl and RNA binding is required for heterochromatin localization of mammalian HP1alpha. EMBO Rep 3:975–981

Nielsen AL, Ortiz JA, You J, Oulad-Abdelghani M, Khechumian R, Gansmuller A, Chambon P, Losson R (1999) Interaction with members of the heterochromatin protein 1 (HP1) family and histone deacetylation are differentially involved in transcriptional silencing by members of the TIF1 family. EMBO J 18:6385–6395

Nielsen AL, Oulad-Abdelghani M, Ortiz JA, Remboutsika E, Chambon P, Losson R (2001) Heterochromatin formation in mammalian cells: interaction between histones and HP1 proteins. Mol Cell 7:729–739

Pacherník J, Bryja V, Ešner M, Kubala L, Dvořák P, Hampl A (2005) Neural differentiation of pluripotent mouse embryonal carcinoma cells by retinoic acid: inhibitory effect of serum. Physiol Res 54:115–122

Rice JC, Allis CD (2001) Histone methylation versus histone acetylation: new insights into epigenetic regulation. Curr Opin Cell Biol 13:263–273

Ryan RF, Schultz DC, Ayyanathan K, Singh PB, Friedman JR, Fredericks WJ, Rauscher FJ III (1999) KAP-1 corepressor protein interacts and colocalizes with heterochromatic and euchromatic HP1 proteins: a potential role for Kruppel-associated box-zinc finger proteins in heterochromatin-mediated gene silencing. Mol Cell Biol 19:4366–4378

Saffery R, Earle E, Irvine DV, Kalitsis P, Choo KH (1999) Conservation of centromere protein in vertebrates. Chromosome Res 7:261–265

Taddei A, Maison C, Roche D, Almouzni G (2001) Reversible disruption of pericentric heterochromatin and centromere function by inhibiting deacetylases. Nat Cell Biol 3: 114–120

Taddei A, Roche D, Bickmore WA, Almouzni G (2005) The effects of histone deacetylase inhibitors on heterochromatin: implications for anticancer therapy? EMBO Rep 6:520–524

Verschure PJ, van der Kraan I, de Leeuw W, van der Vlag J, Carpenter AE, Belmont AS, van Driel R (2005) In vivo HP1 targeting causes large-scale chromatin condensation and enhanced histone lysine methylation. Mol Cell Biol 25:4552–4564

Wakimoto BT (1998) Beyond the nucleosome: epigenetic aspects of position-effect variegation in Drosophila. Cell 93:321–324

Wiblin AE, Cui W, Clark AJ, Bickmore WA (2005) Distinctive nuclear organisation of centromeres and regions involved in pluripotency in human embryonal stem cells. J Cell Sci 118:3861–3868

Wreggett KA, Hill F, James PS, Hutchings A, Butcher GW, Singh PB (1994) A mammalian homologue of Drosophila heterochromatin protein 1 (HP1) is a component of constitutive heterochromatin. Cytogenet Cell Genet 66:99–103

Yamada T, Fukuda R, Himeno M, Sugimoto K (1999) Functional domain structure of human heterochromatin protein HP1(Hsalpha): involvement of internal DNA-binding and C-terminal self-association domains in the formation of discrete dots in interphase nuclei. J Biochem (Tokyo) 125:832–837

Yamaguchi K, Hidema S, Mizuno S (1998) Chicken chromobox proteins: cDNA cloning of CHCB1, -2, -3 and their relation to W-heterochromatin. Exp Cell Res 242:303–314